Primary Castleman's disease in the liver: A case report and literature review

KUN LV[1,2], CHUN-LI ZHANG[3] and MAO-SHENG XU[2]

[1]The First Clinical Medical College, Zhejiang Chinese Medical University; Departments of [2]Radiology and [3]Pathology, The First Affiliated Hospital of Zhejiang Chinese Medical University, Hangzhou, Zhejiang 310006, P.R. China

Received November 23, 2017; Accepted January 31, 2018

DOI: 10.3892/mco.2018.1576

Abstract. Castleman's disease (CD) is a lymphoproliferative abnormality, also referred to as giant lymph node hyperplasia or follicular lymphoid hyperplasia. The occurrence of CD in the liver is rare. Radiological diagnosis of hepatic CD by computed tomography (CT) and magnetic resonance imaging (MRI) remains difficult. On imaging, hepatic CD is often expressed as a single, well-defined soft tissue lesion, with rare cystic degeneration and focal necrosis. The CD lesions appear as hypervascular with abundant cell proliferation on CT and MRI. Polymorphic calcification is commonly identified in the lesion. However, these findings are non-specific for a definitive radiological diagnosis. We herein present a case of hepatic CD and review its pathological and imaging characteristics. In particular, a strip-like area was observed extending from the nodule, which may be helpful for the diagnosis of CD in the liver.

Introduction

Castleman's disease (CD), first described by Castleman in 1954 (1), is commonly encountered in the chest and neck, but is less common in the abdomen and rare in the liver. Primary hepatic CD is very rare, with <20 cases reported in the literature to date (2). Furthermore, description of computed tomography (CT) and magnetic resonance imaging (MRI) characteristics of hepatic CD is rarely found in the radiological literature, particularly from diffusion-restricted on diffusion-weighted imaging (DWI), and CD may be misdiagnosed as a malignant lesion (3). Therefore, the radiological diagnosis of hepatic CD remains difficult. We herein describe a case of hepatic CD detected by CT and MRI, along with a review of the previous cases reported in the literature, with the aim to help improve our understanding and radiological diagnosis of hepatic CD.

Correspondence to: Dr Mao-Sheng Xu, Department of Radiology, The First Affiliated Hospital of Zhejiang Chinese Medical University, 54 Youdian Road, ShangCheng, Hangzhou, Zhejiang 310006, P.R. China
E-mail: xums166@126.com

Key words: Castleman's disease, giant lymph node hyperplasia, liver, computed tomography, magnetic resonance imaging

Case report

An asymptomatic 70-year-old woman underwent a routine physical examination in a local hospital, during which a focal lesion was identified in the right lobe of the liver via ultrasound. The patient received no immediate treatment and was referred for further evaluation to the First Affiliated Hospital of Zhejiang Chinese Medical University (Hangzhou, China). The findings on physical examination and the results of the laboratory tests, including complete blood count and basic metabolic panels, were normal. Subsequently, the patient underwent CT (Somatom, Sensation 64; Siemens, Waltershausen, Germany) and MRI (3.0T Discovery 750; GE Healthcare, Chicago, IL, USA) scans of the abdomen for further evaluation and, finally, the focal lesion was surgically resected.

A non-enhanced abdominal CT was first conducted and revealed well-defined nodular hypoattenuation with punctate hyperattenuation (Fig. 1A, arrow) within a lesion in the eighth segment of the liver. On enhanced CT imaging, the lesion exhibited nodular enhancement (2.3x1.9 cm), and a strip-like enhanced area was found to extend from the nodule in the arterial phase 30 sec after injection of iodine contrast agent (Fig. 1B, arrows), with persistent enhancement in the portal venous phase 65 sec after injection of iodine contrast agent (Fig. 1C).

A follow-up MRI was performed 10 days later and revealed a well-defined nodule (2.6x2.0 cm) with an extended strip in the eighth segment of the liver on T2-weighted imaging. Punctate hypointensity was also observed in the center of the nodule (Fig. 2A, arrow). Both the nodule and the strip displayed hyperintensity on DWI (b=800 sec/mm^2, Fig. 2B) with a low apparent diffusion coefficient (ADC) value ($0.622x10^{-3}$ and $0.693x10^{-3}$ mm^2/sec, respectively; Fig. 2C). Compared with non-enhanced T1-weighted MR images (Fig. 2D), post-contrast MRI revealed significant enhancement of the nodule and the strip in the arterial phase 30 sec after gadolinium injection (Fig. 2E, arrows), and persistent enhancement in the parenchymal phase 120 sec after gadolinium injection (Fig. 2F).

The lesion in the right liver was resected by surgical laparoscopy under general anesthesia. Postoperative pathological examination demonstrated that the pathological components of the nodular mass were lymphocytes and hyalinized vessels

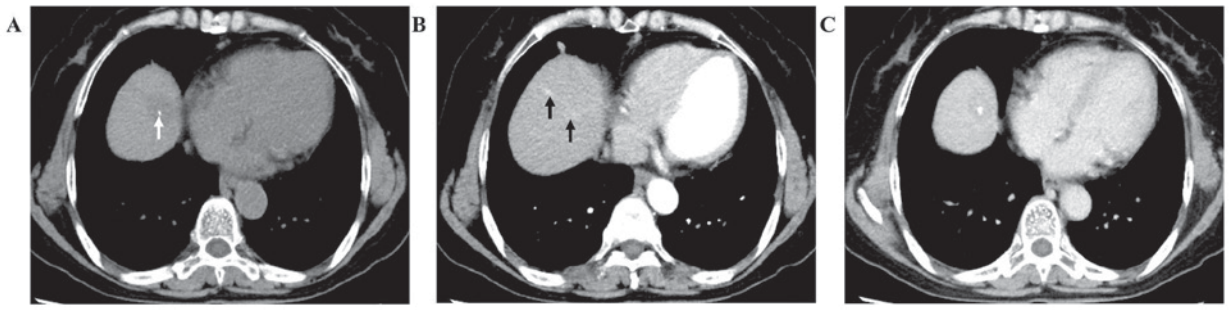

Figure 1. Computed tomography (CT) findings of the lesion. A round nodule with (A) punctate calcification (arrow), (B) mild to intermediate enhancement (arrows) and (C) persistent homogeneous enhancement of the nodule and the strip-like area on pre- and post-contrast CT.

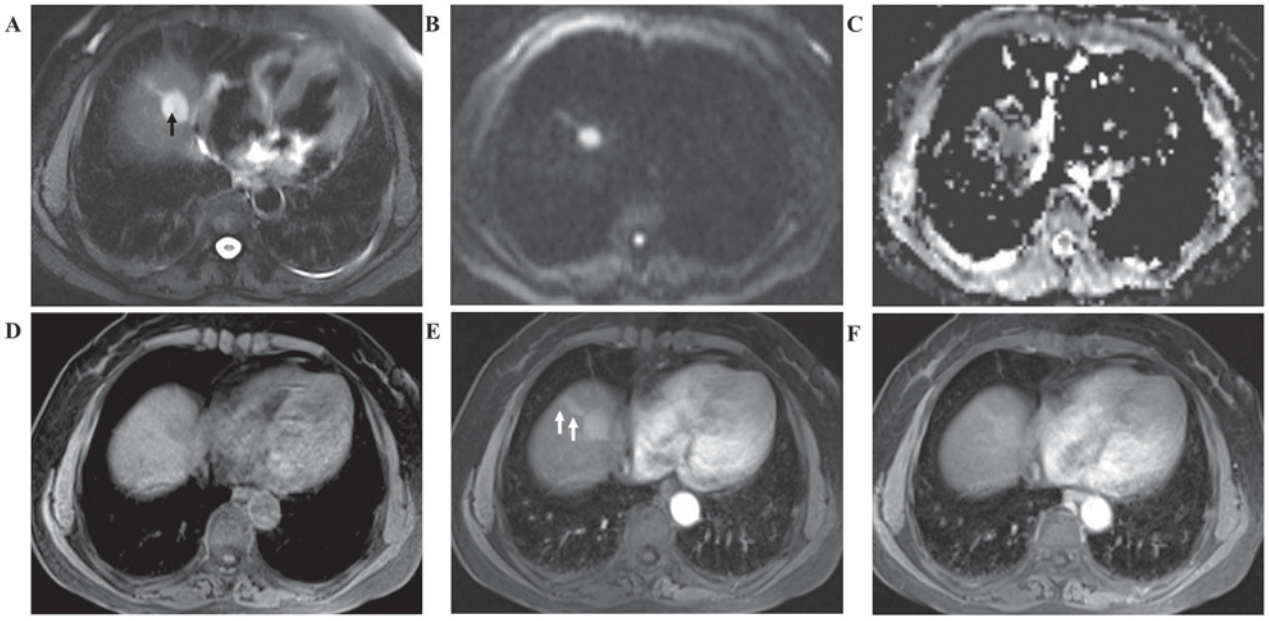

Figure 2. Magnetic resonance imaging (MRI) findings of the lesion. (A) T2-weighted imaging revealed a hypointense nodule with a calcification (arrow). (B) The nodule and the strip displayed diffusion restriction and hyperintensity on diffusion-weighted imaging and (C) a low apparent diffusion coefficient. MRI revealed (D) hypointensity, with (E) significant (arrows) and (F) persistent enhancement of the lesion following contrast administration.

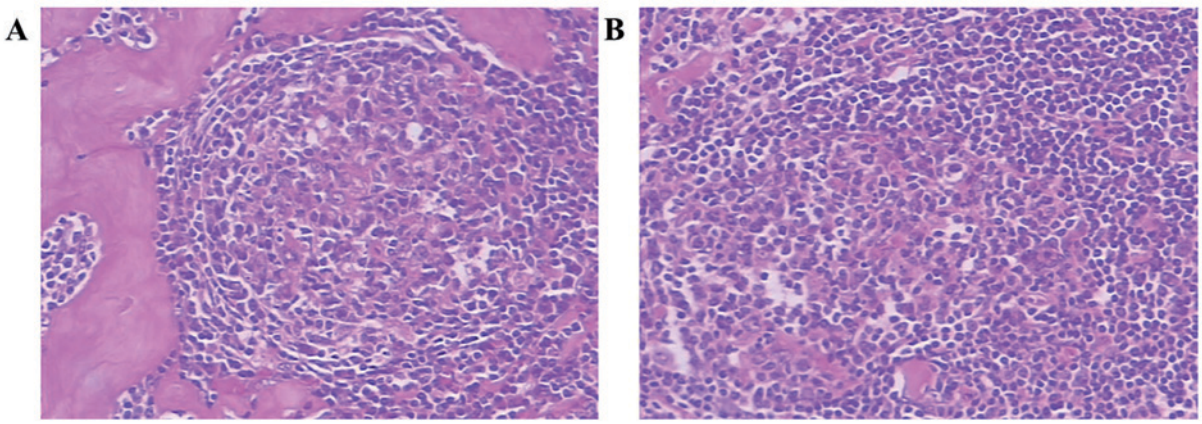

Figure 3. Pathological findings. (A) The nodule was composed of abundant lymphocytes arranged in concentric rings around a germinal center, and hyalinized vessels. (B) The strip-like area was composed mainly of lymphocytes. Hematoxylin and eosin staining (magnification, x400).

(Fig. 3A), with the strip-like area being composed mainly of lymphocytes (Fig. 3B).

Postoperative treatment of the patient was administration with Saimeijie (an atypical β-lactams antibiotic, 2.0 g bid)

Table I. Imaging characteristics of hepatic Castleman's disease.

Authors	Sex/age (years)	Symptoms	Size (cm)	Imaging characteristics			Pathology	(Refs.)
				Margins	Ultrasound	CT/MRI		
Rahmouni *et al*	Female/48	Abdominal pain	5	Well-defined	Hypoechoic	Hypervascular, calcifications	HV	(16)
	Male/28	Asymptomatic	3	Lobulated	Hypoechoic	Hypervascular	HV	
Cirillo *et al*	Female/43	Abdominal pain	13	Well-defined	NA	Nonvascular, calcifications	HV	(17)
Uzunlar *et al*	Female/56	Vague abdominal pain	3.5	Well-defined	Hypoechoic	Hypervascular	HV	(18)
Karami *et al*	Female/5	Abdominal pain	3.7	Lobulated	Solid mass	Hypervascular	HV	(19)
Jang *et al*	Female/40	Abdominal pain, fever and chills	2.2	Well-defined	NA	Hypervascular	HV	(20)
Miyoshi *et al*	Female/70	Asymptomatic	1.5	Well-demarcated	Hypoechoic	Hypovascular	HV	(21)
Dong *et al*	Female/57	Asymptomatic	3.3	Well-defined	NA	Hypervascular, diffusion restricted	HV	(22)
Maundura *et al*	Female/64	Asymptomatic	1.4	Well-defined	Hypoechoic	Hypervascular, diffusion restricted	HV	(23)

HV, hyaline-vascular; NA, not available; CT, computed tomography; MRI, magnetic resonance imaging.

and Ornidazole (0.5 g bid) to prevent infection, and support treatment with hemostasis and rehydration within 2 weeks. Postoperative recovery was good and there has been no recurrence on the last follow-up before the present study was submitted.

Discussion

Castleman's disease (CD) (4) may be histologically divided into hyaline vascular (HV), plasma cell (PC) and mixed variants. The HV variant (5), which is composed of follicles and follicular lymph tissue, is commonly found in women aged 30-40 years and accounts for 90% of diagnosed cases. Phenotypically, this variant is defined by the presence of abundant hyperplastic hyaline capillaries between follicles and lymph sinuses. Furthermore, small lymphocytes in the mantle zone are arranged in concentric rings around the germinal center. The prognosis of the HV variant is mostly favorable following surgical resection. The PC variant (6) is a systemic disease that is more common among patients aged 50-60 years, and accounts for ~10% of diagnosed cases. This variant is defined by enlargement of follicular cells and an abundance of mature plasma cells, but a lower degree of angiogenesis. Treatment is administered systemically using hormone or immunosuppressive agents, but the prognosis of the PC variant is poor. Two clinical subtypes are classified as unicentric CD (UCD) and multicentric CD (MCD) (7-9). UCD occurs most frequently as a focal lesion of the HV variant that is not associated with obvious clinical symptoms and is often incidentally found during routine physical examination. MCD is a systemic disease, with the majority of the cases being of the PC variant, accompanied by systemic symptoms including fatigue, fever, night sweats, weight loss, joint pain and hepatosplenomegaly.

The imaging findings of UCD (10) often present as a single, well-defined soft tissue lesion, with rare cystic degeneration and focal necrosis. This finding may be associated with substantial angiogenesis and development of an extensive collateral circulation, so the lymph follicle tissue is not prone to necrosis (11). Non-enhanced CT images revealed homogeneous mild hypoattenuation within the lesion. Non-enhanced MR T1WI revealed a slightly hyperintensity compared with muscle. Furthermore, T2WI and DWI displayed high signals, suggesting diffusion restriction and supporting abundant cell proliferation (12). Contrast-enhanced CT/MRI of CD lesions often displays mild to moderate enhancement during the arterial phase, and persistent enhancement during the venous phase (13). This finding may be associated with the small arterial lumen and the subsequent reduction in blood velocity. Polymorphic calcification is commonly found in the lesions (14), which may be attributed to capillary proliferation with wall thickening and accompanied by glassy degeneration, fibrotic degeneration and the formation of calcareous deposits along the vessel wall. Imaging findings in MCD (15) include multiple enlarged lymph nodes with homogeneous density and mild to moderate enhancement on a contrast-enhanced scan, which pathologically reflects enlarged follicles and follicular plasma cell infiltration. In MCD is of the HV variant, the degree of enhancement is similar to that of UCD.

The reported imaging findings of hepatic CD (16-23) (Table I) are commonly consistent with UCD. These findings and the calcification of the lesion may be helpful for radiological diagnosis of CD in the liver. Moreover, we observed

that the signal, density, and pathological components of the strip-like area were consistent with those of the nodule. To the best of our knowledge, this finding has not been previously reported in the literature on hepatic CD to date. We hypothesized that the strip-like area may be attributed to lymphoid tissue, and lymphoproliferative disease may develop anywhere where lymphoid tissue is present (20). This strip-like area extending from the nodule may help with the differential diagnosis of hepatic CD from other diseases. However, pathological examination is required for a definitive diagnosis.

Acknowledgements

Not applicable.

Funding

No funding was received.

Availability of data and materials

The datasets used and/or analyzed during the current study are available from the corresponding author on reasonable request.

Competing interests

The authors declare that they have no competing interests.

Ethics approval and consent to participate

This article does not contain any studies with human participants or animals performed by any of the authors.

Authors' contributions

All authors contributed to this paper and approved the final version. LK wrote the case report. ZCL offered the assistance for the pathologic diagnosis of this case. XMS and LK revised and edited the final version.

Consent for publication

The patient and/or her family consented to the publication of the case details and associated images.

References

1. Castleman B and Towne VW: Case records of the massachusetts general hospital; weekly clinicopathological exercises; founded by Richard C. Cabot. N Engl J Med 251: 396-400, 1954.
2. Talat N, Belgaumkar AP and Schulte KM: Surgery in Castleman's disease: A systematic review of 404 published cases. Ann Surg 255: 677-684, 2012.
3. Malayeri AA, El Khouli RH, Zaheer A, Jacobs MA, Corona-Villalobos CP, Kamel IR and Macura KJ: Principles and applications of diffusion-weighted imaging in cancer detection, staging, and treatment follow-up. Radiographics 31: 1773-1791, 2011.
4. Soumerai JD, Sohani AR and Abramson JS: Diagnosis and management of Castleman disease. Cancer Control 21: 266-278, 2014.
5. Keller AR, Hochholzer L and Castleman B: Hyaline-vascular and plasma-cell types of giant lymph node hyperplasia of the mediastinum and other locations. Cancer 29: 670-683, 1972.
6. Ferry JA and Harris NL: Atlas of lymphoid hyperplasia and lymphoma. WB. Saunders Company: 99-1042, 1997.
7. Gaba AR, Stein RS, Sweet DL and Variakojis D: Multicentric giant lymph node hyperplasia. Am J Clin Pathol 69: 86-90, 1978.
8. Casper C: The aetiology and management of Castleman disease at 50 years: Translating pathophysiology to patient care. Br J Haematol 129: 3-17, 2005.
9. van Rhee F, Stone K, Szmania S, Barlogie B and Singh Z: Castleman disease in the 21st century: An update on diagnosis, assessment, and therapy. Clin Adv Hematol Oncol 8: 486-498, 2010.
10. Zhou LP, Zhang B, Peng WJ, Yang WT, Guan YB and Zhou KR: Imaging findings of Castleman disease of the abdomen and pelvis. Abdom Imaging 33: 482-488, 2008.
11. McAdams HP, Rosado-de-Christenson M, Fishback NF and Templeton PA: Castleman disease of the thorax: Radiologic features with clinical and histopathologic correlation. Radiology 209: 221-228, 1998.
12. White NS, McDonald C, Farid N, Kuperman J, Karow D, Schenker-Ahmed NM, Bartsch H, Rakow-Penner R, Holland D, Shabaik A, *et al*: Diffusion-weighted imaging in cancer: Physical foundation and application of restriction spectrum imaging. Cancer Res 74: 4638-4652, 2014.
13. Jiang XH, Song HM, Liu QY, Cao Y, Li GH and Zhang WD: Castleman disease of the neck: CT and MR imaging findings. Eur J Radiol 83: 2041-2050, 2014.
14. Bonekamp D, Horton KM, Hruban RH and Fishman EK: Castleman disease: The great mimic. Radiographics 31: 1793-1807, 2011.
15. Johkoh T, Müller NL, Ichikado K, Nishimoto N, Yoshizaki K, Honda O, Tomiyama N, Naitoh H, Nakamura H and Yamamoto S: Intrathoracic multicentric Castleman disease: CT findings in 12 patients. Radiology 209: 477-481, 1998.
16. Rahmouni A, Golli M, Mathieu D, Anglade MC, Charlotte F and Vasile N: Castleman disease mimicking liver tumor: CT and MR features. J Comput Assist Tomogr 16: 699-703, 1992.
17. Cirillo RL Jr, Vitellas KM, Deyoung BR and Bennett WF: Castleman disease mimicking a hepatic neoplasm. Clin Imaging 22: 124-129, 1998.
18. Uzunlar AK, Ozateş M, Yaldiz M, Büyükbayram H and Ozaydin M: Castleman's disease in the porta hepatis. Eur Radiol 10: 1913-1915, 2000.
19. Karami H, Sahebpour AA, Ghasemi M, Karami H, Dabirian M, Vahidshahi K, Masiha F and Shahmohammadi S: Hyaline vascular-type Castleman's disease in the hilum of liver: A case report. Cases J 3: 74, 2010.
20. Jang SY, Kim BH, Kim JH, Ha SH, Hwang JA, Yeon JW, Kim KH and Paik SY: A case of Castleman's disease mimicking a hepatocellular carcinoma: A case report and review of literature. Korean J Gastroenterol 59: 53-57, 2012.
21. Miyoshi H, Mimura S, Nomura T, Tani J, Morishita A, Kobara H, Mori H, Yoneyama H, Deguchi A, Himoto T, *et al*: A rare case of hyaline-type Castleman disease in the liver. World J Hepatol 5: 404-408, 2013.
22. Dong A, Dong H and Zuo C: Castleman disease of the porta hepatis mimicking exophytic hepatocellular carcinoma on CT, MRI, and FDG PET/CT. Clin Nucl Med 39: e69-e72, 2014.
23. Maundura M, Hayward G, McKee C and Koea JB: Primary Castleman's disease of the liver. J Gastrointest Surg 21: 417-419, 2017.